PROCEEDINGS, Fourtieth Workshop on Geothermal Reservoir Engineering
Stanford University, Stanford, California, February 22-24, 2016
SGP-TR-209

Quantifying Surface Roughness to Detect Geothermal Manifestations from Polarimetric Synthetic Aperture Radar (PolSAR) Data

Asep Saepuloh[1], Katsuaki Koike[2], Mohamad Nur Heriawan[1], and Taiki Kubo[2]

[1]Bandung Institute of Technology (ITB), Jl. Ganesha No. 10, Bandung 40132, Indonesia.

[2]Graduate School of Engineering, Kyoto University, Katsura C1-2-215, Kyoto 615-8540, Japan.

E-mail address saepuloh@gc.itb.ac.id

Keywords: Surface roughness, PolSAR, ALOS PALSAR, geothermal, Wayang Windu

ABSTRACT

Spatial mapping of geothermal-resource potential with an accurate detection of steam spot using remotely-sensed technology requires quantification of physical parameters of surface manifestation related to geothermal system. Synthetic Aperture Radar (SAR) remote sensing, the only useful observation and monitoring technology that can be undertaken in any weather condition, measures backscattering powers returned to a satellite sensor. The backscattering is mainly controlled by the surface roughness that is related to rock types. Resistance to the geological processes such as weathering, erosion, and alteration is different with rock type, which causes a dependence of the surface roughness upon rock type. The backscattering is also affected by dielectric permittivity and magnetic permeability of the ground surface. The purpose of this study is to develop methods for quantifying the surface roughness from the SAR data and detecting surface manifestations of geothermal based on the roughness. A surface roughness dataset by ground-truthing in a geothermal field using a profiler of 30 cm length was used to verify the estimated roughness. Detrending and interleaving techniques of the surface profile were applied to quantify accurately the surface roughness. Correlations of the measured surface roughness with the polarized backscattering intensity and the incidence angle were investigated, which was finally used to make a physical model by a curve fitting of 269 data points. The resultant model was applied to map a spatial distribution of the surface roughness over a 72 km^2 area in the Wayang Windu geothermal field, West Java, Indonesia using two scenes of Full Polarimetric mode of the Phased Array L-band Synthetic Aperture Radar (PALSAR) onboard Advanced Land Observing Satellite (ALOS). Both the ground-truthing and the SAR roughness data indicated that the roughness increased and decreased gradually towards the altered surface manifestations. The rock types and thermal intensities of hydrothermal fluid controlled the surface roughness in general. For lava and pyroclastic rocks, hydrothermal fluids have altered the rock matrices into clay minerals that are easily eroded. The rock fragments are more resistant than rock matrices at ground surfaces. Consequently, surface of the altered rocks becomes rough than the intact rocks in general. For tuff and lahar deposits, hydrothermal fluids have altered all the rock compositions into clay minerals and produced flat surfaces.

1. INTRODUCTION

Characterizing physical properties of ground surface using Synthetic Aperture Radar (SAR) are crucial for geological target detection under Torrid Zone condition (Saepuloh et al., 2010). The backscattering intensity of SAR chiefly is a function of two physical quantities of surface material, surface roughness and dielectric parameter. The two parameters were proved effective to discriminate ground surface materials at volcanic field such as pyroclastic flows, lava, and lahars (Saepuloh et al., 2010). In this paper, we focused on the surface roughness parameter at geothermal field because this parameter controls the backscattering signals significantly (e.g. Duarte et al., 2008; Saepuloh et al., 2012; Saepuloh et al., 2015). The surface roughness discussed in this paper means the variance of Earth surface elevations above the horizontal line. The interaction between hydrothermal fluid and host rocks is aimed to be analyzed by the surface roughness parameter. The resistance of the rocks presented by their roughness to the geological processes such as alteration due to geothermal process depends on rock type and/or thermal intensity.

Planetary surface roughness extraction and modelling using remotely sensed techniques is one of challenging topics for the last decades. The surface roughness is one parameter that geological features could be predicted such as topographic feature associated with lava flows (Campbell, 1996) and soil (Duarte, 2008). Typical quantifying techniques are template devices, stereo-photography, simple surveying, laser altimetry, and radar interferometric (Campbell and Garvin, 1993). However, quantitative interpretation of data collected in fields is still a difficult problem. The main problem in analyzing such data is how to quantify the surface roughness for comparison with radar observation and prediction of backscatter behavior in various polarization modes. To overcome this problem, we measured surface roughness at a field along three directions: azimuth, range, and dominant topographic undulation. The azimuth and range directions follow the satellite movement and line of sight, respectively. The dominant topographic undulation is a general pattern of topography within 30 m radius. A fixed pin meter with correlation length 30 cm, similar to the L-band frequency, was used for the measurement. The polarimetric mode of the Phased Array Synthetic Aperture Radar (PALSAR) onboard Advanced Land Observing Satellite (ALOS) were used in this study. In order to obtain the most representative ground surface model, a combination of the backscattering intensity data for each polarization mode and directional surface roughness at field was analyzed. The linear curve fitting method was applied to approximate the measured surface roughness at field using Polarimetric SAR data. The surface roughness was measured at 269 points at field along above the three directions. The surface roughness was identified for three geothermal manifestation zones, altered surfaces, mud pools, and hot springs in the selected study area of Mt. Wayang Windu, situated in the southern part from Bandung City, West Java, Indonesia (Fig. 1).

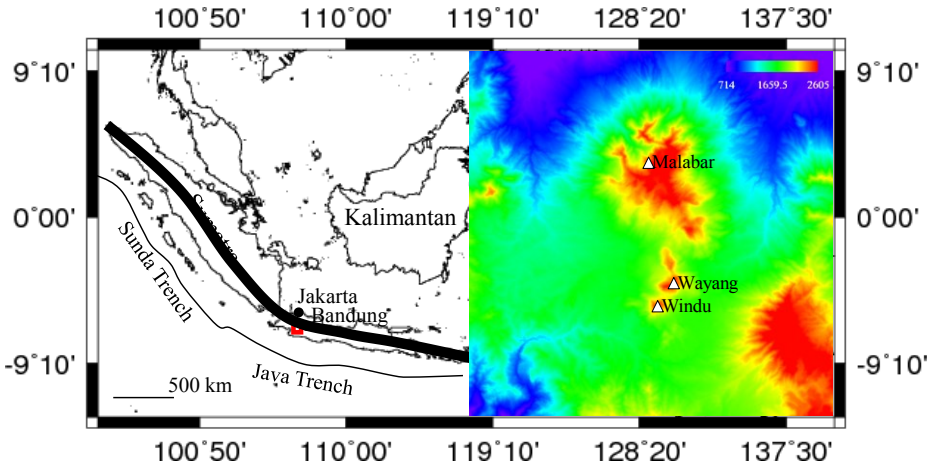

Figure 1: Study area located at Mt. Wayang Windu in West Java, Indonesia with sites of explored geothermal prospects in gray arc segments (Hochstein and Sudarman, 2008). Inset showing local topographic of study area presented by SRTM 30 m DEM (Farr et al., 2007).

Mt. Wayang Windu in a part of volcanic arc was formed in response to the subduction of the Australian–Indian Plate beneath the Eurasian Plate. This subduction has been active since Cretaceous (Whittaker et al., 2007).

2. DATA ACQUISITION AND MEASUREMENTS

Two scenes polarimetric ALOS PALSAR data level 1.5 in multilook geocoded were used to analyze backscattering behavior of the ground surface roughness. We selected dataset with similar incidence angle to avoid a bias originated from the difference in off nadir of the two data. The backscatter or power returned to the radar antenna from a certain area at surface is expressed by backscattering coefficient σ^0. Following Saepuloh et al. (2015) the σ^0 can be quantified from ALOS PALSAR data based on physical parameters as follows:

$$\sigma^0_{\eta\xi} = \left(4k^4 {h_0}^2 \cos^4\theta_i\right)\left|\alpha_{\eta\xi}\right|^2 \omega \quad (1)$$

where η and ξ denote the scattered and incident polarization modes, respectively, in either the horizontal (H) or vertical (V) direction; k is the wave number; h_0 is the height of a random surface above the mean plane or surface roughness; θ_i is the angle of incidence from the mean normal direction to the surface; ω is the roughness height spectral density of the surface; and α is electrical parameter of the surface. Since the h_0 should be constant at surface, we tried to accommodate the roughness model by four polarized modes: HH, HV, VH, and VV. The HH and VV termed as co-polarization and HV and VH as cross-polarization are analyzed based on field roughness measurements.

For field surface roughness, we measured the surface roughness using a set of pin meters at the geothermal manifestations. There are nine zones identified as geothermal manifestation including hot springs, fumaroles, mud pools, and alteration zones. The gridded measurements about 30 m lag were performed at the nine zones to obtain detail transition of hydrothermal activity to the surface roughness spatially. There is a large crater rim about 3.3 km in diameter with two highest summits at the northern and southern rims termed as Puncak Besar and Malabar. Southern part from the rim separates the other summits, termed Gambung, Bedil, Wayang, Windu, and Ramiru. Generally, the summits are distributed from north to south and Wayang Windu is located in the middle summit lines. The measured points are distributed around the summit lines. There are three measured crater zones containing surface manifestation to be discussed in the following section. The three measured zones are located between Puncak Besar and Gambung with mud pools manifestations, Bedil and Wayang by altered surfaces manifestation. Their locations are simply termed Zone-1 and 2. The Zone-3 was selected at hot springs manifestations about 4 km from the craters. The surface roughness at the three Zones were identified and compared for the σ^0 from co- and cross polarization modes.

Variety techniques to measure surface roughness at filed have been discussed. Campbell and Garvin (1993) used laser profilers, Gaddis et al., (1993) used mechanical profiler, and Farr (1992) used stereo-photography to measure surface roughness. Their investigated profile lengths are also varying from centimeters to hundred meters. The longer profile length produced generalization effect when root-mean-square (RMS) roughness base quantification is used. A physical measures approach was adopted in this paper to quantify surface roughness using a fixed 30 cm pin meter. This approach produces a realistic quantitative characterization of natural terrain by taking an assumption that the surface is stationary (Shepard et al., 2001). Investigated profile length is 30 cm to obtain surface roughness in detail based on RMS roughness criterion. This length is also agreeable with sensitivity of L-band frequency to distinguish surface materials based on their roughness (Saepuloh et al., 2013). In order to know the backscatter response to the surface roughness in azimuth and range direction, we measured surface roughness at field along flight direction of the SAR sensor (azimuth), look direction (range), and dominant topographic undulations termed as N-S, E-W, and N to E. The dominant topographic undulation was also observed because at certain areas the roughness does not align to the azimuth and roughness.

The field roughness measurements permit to establish three qualitative classes of geothermal surface manifestation: alteration zones, mud pools, and hot springs. In this paper, the discussion is focused on the surface roughness characteristics at the three classes: Zone-1, 2, and 3. Zone-1 located between Bedil and Windu is composed by altered surfaces, Zone-2 between Puncak Besar and Gambung is composed by mud pools, and Zone-3 is composed by hot springs. The selected zones are presenting general geothermal surface manifestation at Wayang Windu geothermal field. The ground surface of Zone-1 located at Wayang Crater is composed by vegetation, grasses, and fragmental rocks with size 5 – 30 cm. The rock surface generally has been altered to be soil with bright greyish to yellowish color. The vegetation is rare at alteration areas. Zone-2 located at Burung Crater is composed mainly by dense vegetation, grasses, and farms. The ground surface is composed chiefly by flat soils with mud pools at the crater area. Zone-3 located at Kertamanah is composed by grasses, farms, and ponds. The tea plantations are also existed at hilly terrain. The hot springs deliberate warm water about 55° C with pH 6.3 to the ponds. The ground surface is dominated by the almost flat soils and grasses.

3. SURFACE ROUGHNESS QUANTIFICATION AND GEOTHERMAL ASSESSMENT

The pin meter measures different pin height of topographical expression in centimeter scale. To quantify the surface roughness, some parameter presenting the roughness could be calculated statistically from correlation of each pin height. The common parameters used are slope and offset power spectra, root-mean-square (RMS) height, and RMS slope (Campbel and Shepard, 1996). In this paper, we used RMS height H_0 of detrended profile to quantify surface roughness from the pin meter reading. The H_0 was calculated for N-E, E-W, and N to E measurement directions as follows:

$$H_0(\zeta) = \sqrt{\left[\frac{1}{n}\sum_{i=1}^{n}(z(x_i) - \bar{z})^2\right]_{\zeta}} \tag{2}$$

where n is number of pin bar (=60), $z(x_i)$ is height of the surface at point x_i, $\bar{z}$ is mean height of the surface within the profile, and ζ is measurement direction either in N-S, E-W, or N to E.

Following roughness quantification standard by Shepard et al. (2001), we used detrending and interleaving process to the original data. The detrending process was applied using a best fit line subtraction of the original data to produce zero mean of the profile. This process is used to emphasize the small scale variation of terrain from general trend. The detrending process was also proved effective to reduce topographic effect from roughness component within the profile. Figure 2 shows the detrending performance to the original data at the selected measurement point WW-020. The detrended surface roughness presented in three directions: N-S, E-W, and N 115º E produced the terrain profile with zero mean. Each measurement direction produced topographic expression of surface roughness. Based on this plot, we obtained that the surface roughness is not only function of topographic expression, but also the measurement direction. Therefore, three dimensional measurements are necessary to quantify precise surface roughness parameter. The interleaving process was also applied to the RMS height H_0 to obtain accurate correlation each pin height in a profile. The process is a technique which two pin points on a surface are chosen and compared. Thus, the process is effective to reduce dependencies of H_0 to the profile length. Therefore, the quantified surface roughness is predicted representing the wide terrain not only a measured point.

Assessing the geothermal manifestation, we tried to correlate the H_0 explained in the previous to the acidity parameter at and around surface manifestations. The acidity parameter presented by pH lower than 7 is one parameter to identify geothermal surface manifestation (Libbey and Williams-Jones, 2016; Gherardi et al., 2002; Joseph et al., 2013). There were three zones identified based on geothermal manifestation types: Zone-1 at altered surfaces, Zone-2 at mud pools, and Zone-3 at hot springs areas. The correlation plot was depicted by Figure 3 for each zone with three directions of measurement: N-S, E-W, and N to E. According to the plot, there is a separation at pH 5 that the plots are concentrated at lower and higher than pH 5. The separation is originated from discrete surface manifestation zone. There is no gradational pH in spatial boundary of surface manifestation. It may infer that the surface manifestation is local and the thermal effect from geothermal fluids affect the ground surface locally.

For Zone-1, pH higher than 5 correlated with low H_0 and lower than 5 with high H_0. A medium correlation determination about 0.5 was obtained by the mean of the three directions of measurement. According to the geological map of Alzwar et al. (1992), Zone-1 is composed by altered lava and pyroclastics from Malabar old volcanic products.

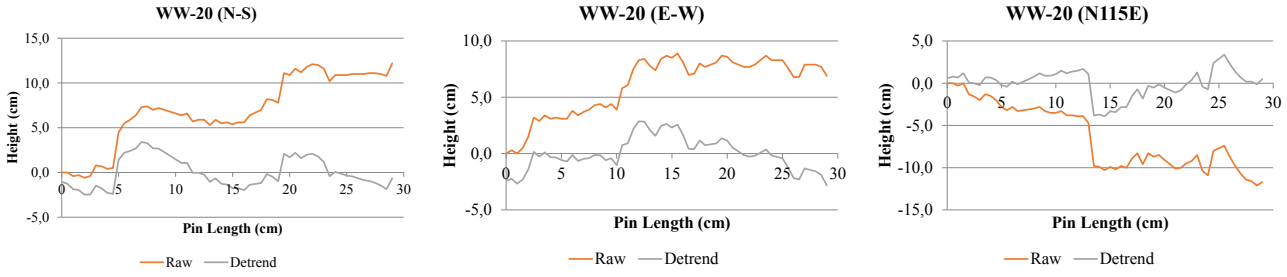

Figure 2: Detrending process at one point at Zone-1 as shown by Figure 2 to remove the topographic effect in the surface roughness measurements.

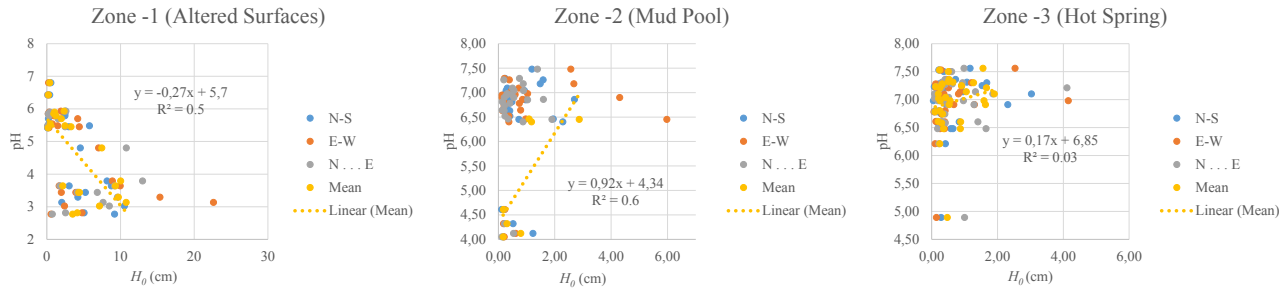

Figure 3: Scatterplot between RMS surface roughness and pH at different geothermal surface manifestation showing the characteristics of ground surface due to hydrothermal activities. Surface roughness measurements at field were performed in three directions N-S, E-W, and N to E to obtain complete parameter of surface roughness. The mean values among the three were used to calculate the correlation determination with pH.

We interpreted that the geothermal fluids affected to the rock matrices of lava and pyroclastics is higher than rock fragments. Therefore, the altered rock matrices are easier to be eroded than rock fragments. The field observation confirmed that the ground surfaces are covered chiefly by rock fragments with size from gravel to boulder. Low pH caused strong alteration to the matrices of lava and pyroclastics which produced rough surfaces from rock fragments. On the contrary, high pH affects the rock surfaces relatively weak for same geological condition.

For Zone-2, a higher correlation determination about 0.6 than altered surfaces at Zone-1 was obtained. According to the geological map of Alzwar et al. (1992), Zone-2 is composed by Malabar volcanic products containing tuff and laharic breccia. The low and high pH are located at low and high H_0, respectively. Contrary to the altered surfaces, the smooth and rough surfaces agreed with low and high pH, respectively. The ground surface of Zone-2 located at Burung crater is covered by rare vegetation such as grasses, farms, and trees around the crater. The crater with diameter about 350 m is bordered by abrupt topographic at NE part and located in the valley with flat surfaces in general. Based on field condition, the weathering is more influence to the ground surfaces than alteration process. We interpreted that the weathering process changes the rock matrices and fragments to soil. Therefore, the ground surface is flat without fragmental material such as gravel and boulder.

The correlation between pH and H_0 at Zone-3 showed a discrepancy. The low correlation about 0.03 was obtained from the scatterplot. The ground surface of Zone-3 is covered by grasses, tea plantations, and farms. The hot springs are located at wet ground and ponds with undulated topography. The temperature and pH of the warm ponds are about 55º C and 6.3, respectively. The hot springs might affect the host rocks weakly. Therefore, surface roughness is independently to the spatial effect of the hot springs. According to the geological map of Alzwar et al. (1992), Zone-3 is composed by laharic deposits containing fine to coarse old volcanic products. The weak and limited hydrothermal activities to a large fragmented materials might cause low correlation between pH and the surface roughness. According to characteristics of the surface roughness at three geothermal manifestation zones, we identified that the altered surfaces and mud pools have correlation to the roughness of their ground surfaces. The rock types and thermal activities are supposed to be the significant to the surficial processes. Strong thermal activities will alter the matrices of hard volcanic products such as lava flow and pyroclastics into high erodibility material such as clays. Then, the erosional process removes the matrices and remains the fragments of the rocks. Therefore, the surface roughness will be high. However, when the high thermal activities interact with soft volcanic products such as tuff and lahar, the surface erodibility will be high which produces flat surfaces. It may infer that the low thermal activities will affect the volcanic products weakly. Therefore, the surface roughness is independent to the surface geothermal manifestation. Following this characterization and identification, we tried to generate a surface roughness model using polarimetric ALOS PALSAR and surface roughness measured at altered surfaces. Spatial surface roughness model should provide a possibility to detect altered surfaces widely as discussed in the next section.

4. BACKSCATTERING POLARIMETRIC SAR RESPONSE TO THE SURFACE ROUGHNESS

Backscattering of SAR data is known to be an effective means of assessing surface roughness and the dielectric property of surface material (e.g., Evans et al., 2012; Saepuloh et al., 2015). However, interaction between surface roughness and polarized backscattering signal is still unclear. We used two scenes data of ALOS PALSAR data as explained in. The ALOS PALSAR is utilized by capability to transmit and receipt signals in horizontal (H) and vertical (V) propagation. Therefore, once acquisition produced four polarized composition termed as HH, HV, VH, and VV. The co- and cross-polarization were used to simplify explanation for HH-VV and HV-VH, respectively. Following Saepuloh et al. (2015), we quantified the backscattering intensity by taking the logarithmic scale of the multi-look data. The range of backscattering intensity values in dB unit for co-polarization is wider than cross-polarization images. For co-polarization mode, the backscattering intensity is about -1 to 7 dB and cross polarization mode is about 0 to 6 dB. More features with low backscattering intensity were detected by cross- than co-polarization mode. Various physical properties and/or geometry of surface materials are predicted responsible to detected features. Measurement direction of surface roughness, radar geometry, and polarization mode are the main issue to be discussed in this section on how the surface roughness at field responses to the radar backscattering in range and azimuth direction.

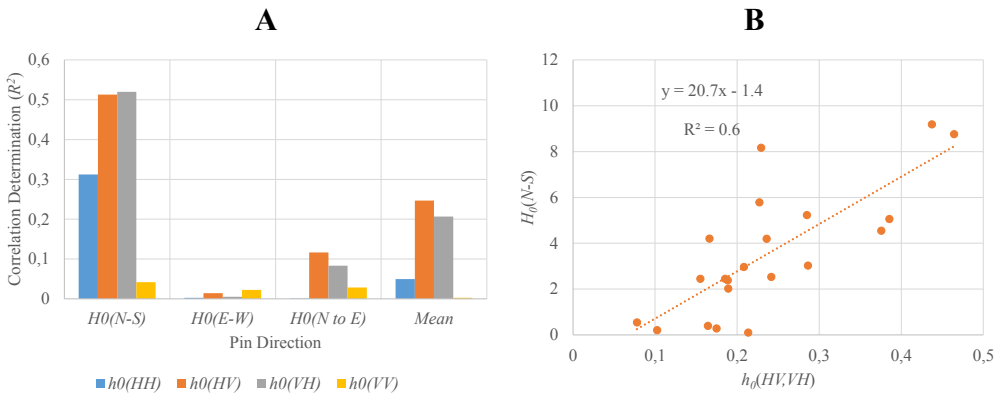

Figure 4: North-south roughness measurements in cross-polarization modes showing higher correlation than the other measurement direction and co-polarization mode (A) and scatterplot of roughness model derived from field roughness measurement showing the highest correlation using HV and VH simultaneously.

The initial surface roughness model was used as basis sensitivity identification to the surface roughness at the field. According to Saepuloh et al. (2015), the model could be calculated for each polarization type as follows:

$$h_0(\eta\xi) = \lambda \sqrt{-\frac{1}{60}\ln\left(1 - \frac{10^{\left(0.1\times\sigma^0_{\eta\xi}\right)}}{0.04\cos\theta_i}\right)} \tag{3}$$

where $h_0(\eta\xi)$ is surface roughness model based on polarized mode, $\eta\xi$ is polarized mode either in H and V, $\sigma^0_{\eta\xi}$ is backscattering coefficient on polarized mode, and θ_i is local incidence angle.

The linear fitting methods were used to obtain correlation determination R^2 between surface roughness at field H_0 and model h_0. Figure 4A shows the linear fitting result regarding polarization modes and measurement directions. The highest R^2 were obtained by surface roughness model from cross-polarization modes except in the E-W measurement direction. Regarding the measurement directions, the N-E measurement with cross-polarization is the highest R^2 about 0.5. The N-E measurement agreed to the radar flight direction or azimuth provided highest correlation of surface roughness. Therefore, we used the N-E measurement with backscattering of cross-polarization mode to improve the initial h_0. Improving the h_0, we tried to accommodate the HV and VH polarized mode to the initial model as depicted by equation 3. The linear fitting method with R^2 was used as the optimum criterion to the h_0. The linear fitting for selecting the best fit model was depicted by Figure 4B. The obtained R^2 of the h_0 with single polarization mode was only less than 0.5. To improve surface roughness model, we used combination of polarization mode HV and VH. The optimum model with R^2 about 0.6 is depicted by Figure 4B and written as follows:

$$h_0(HV,VH) = \left(h_0^2(HV) + h_0^2(VH)\right) \times e^{\theta_i^3} \times 10^{\cos\theta_i^7} \tag{4}$$

where $h_0(HV,VH)$ is surface roughness model using HV and VH polarized mode, $h_0(HV)$ and $h_0(VH)$ are surface roughness function based on eq. 3 for σ^0_{HV} and σ^0_{VH}, respectively.

The spatial surface roughness model was calculated using a Triangulated Irregular Network (TIN) gridding method as depicted by Figure 5 (2nd row). We identified and simplified explanation for the rough, medium, and smooth surfaces with RMS height more than 10, about 8, and less than 8 cm, respectively. The RMS height of surface roughness between the model and field data agreed in general. According to the field data, the gradational surface roughness from rough to smooth surface is located at south to northwest part. The subset images of pH measurement and surface roughness model at the three geothermal surface manifestation zones is depicted by Figure 5.

For Zone-1, the spatial distribution of low pH agreed to the rough surface roughness. The high resistance of the rock fragments than rock matrices to the hydrothermal fluid caused the ground surface is composed chiefly by material in gravel and boulder size. The volcanic products from lava and pyroclastics were responsible the roughness of altered surfaces. For Zone-2, the smooth surfaces are located at northeast part and agreed with low and medium pH as presented by point from WW25 to WW29. The hydrothermal interaction with tuff and laharic breccia caused the surface of mud pool zones is flat. The very smooth surfaces distributed sparsely at NW and SE are predicted from strong weathering process. For Zone-3, the smooth surfaces are located at southeast and west, respectively. The hot springs are located at very smooth surface as presented by low pH at WW60, WW61, and WW71. The interaction between hydrothermal fluids and fine to coarse old volcanic products at Zone-3 is responsible to the flattering of the surfaces. Moreover, the intensive weathering process might be also caused the surface is flat. Therefore, the effect of alteration and weathering are presented by very smooth surfaces at hot springs zones.

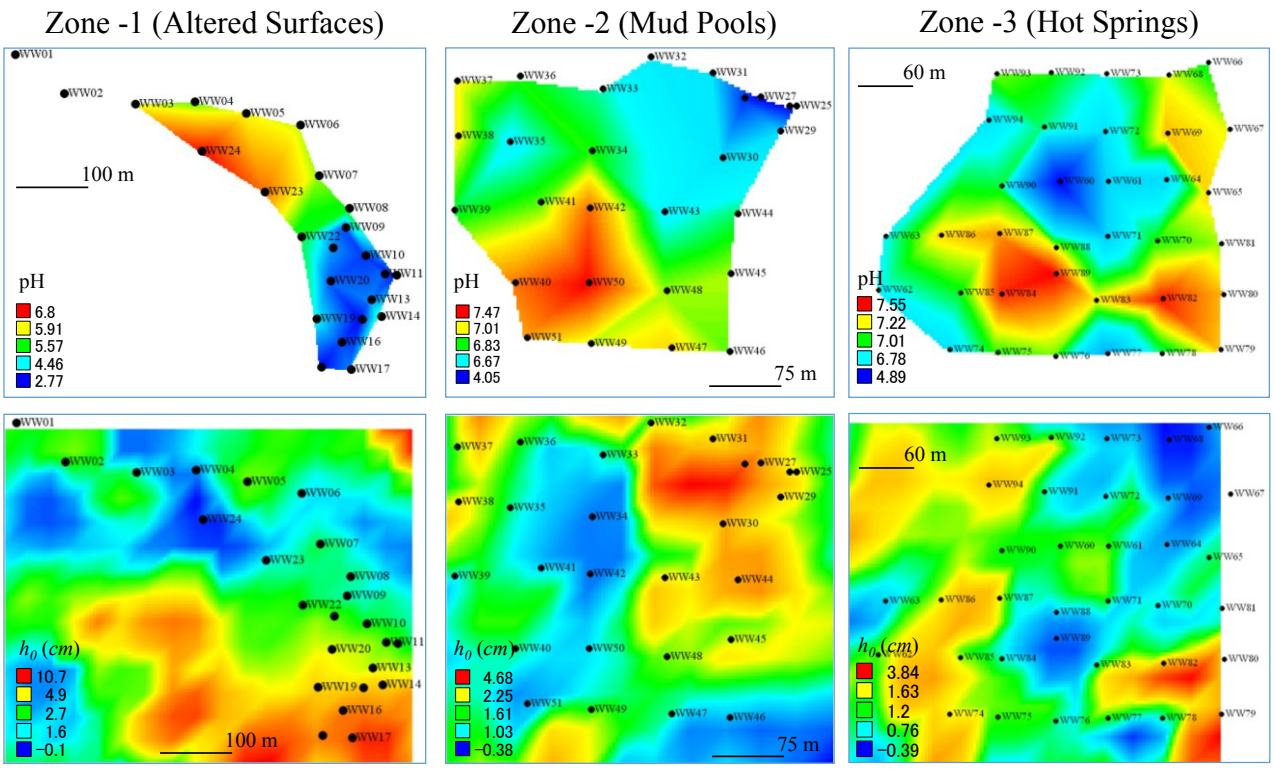

Figure 5: Spatial distribution of pH and surface roughness model obtained from cross-polarization modes for Zone-1 (altered surfaces), Zone-2 (mud pools), and Zone-3 (hot springs). Black dots area ground measurement points at the three zones.

5. CONCLUSIONS

The physical properties of surface manifestation including acidity and surface roughness at geothermal field could be identified successfully. The acidity shown by lower pH than 7 at geothermal surface manifestations revealed a constant pattern in general that the lowest pH is located at and around surface manifestations. The separated plots between high and low pH were originated from thermal features in that the surface manifestation is local and the thermal effect from geothermal fluids affect the ground surface locally. Detrending and interleaving techniques were applicable for surface roughness measurements in cm scale. The techniques could quantify RMS height of surface roughness by emphasizing the small scale variation of terrain from general trend reducing topographic effect from roughness component within the profile. For the surface roughness, the geothermal surface manifestations were classified into altered surfaces, mud pools, and hot springs. The highest correlation between surface roughness and acidity was provided at the altered surfaces with volcanic products such as lava and pyroclastics, and mud pools with tuff and lahars. The discrepancy was shown by hot springs surfaces with laharic deposits containing fine to coarse old volcanic products. The rock types and thermal activities were significant to the surface roughness condition. The surface roughness model could be estimated based on Polarimetric Synthetic Aperture Radar (PolSAR) data from the Phased Array Synthetic Aperture Radar (PALSAR) onboard Advanced Land Observing Satellite (ALOS). The N-S field roughness measurements at altered surfaces provided the best correlation with the backscattering of cross-polarization, HV and VH modes. The azimuth or flight direction of the ascending satellite was influenced to the detected roughness in the cross-polarization mode. According to the field data and model, the low pH coincided to the rough surfaces at altered surfaces and the smooth surfaces at mud pools.

ACKNOWLEDGMENTS

The authors wish to thank “Beneficial and Advanced Geothermal Use System (BAGUS)” project in the Science and Technology Research Partnership for Sustainable Development (SATREPS) and the Institute for Research and Community Services of ITB for fully supporting this cooperative research.

REFERENCES

Alzwar, M., Akbar, N., and Bachri, S.: Geological map of the Garut and Pameungpeuk Quadrangle, Jawa scale 1:100,000, *Geological Research and Development Centre Indonesia*, (1992).

Campbel, B.A. and Shepard, M.K.: Lava flow surface roughness and depolarized radar scattering, *Journal of Geophysics Research*, **101** (E8), (1996), 18,941 - 18,951.

Campbel, B.A. and Garvin, J.B.: Lava Flow Topographic Measurements for Radar Data Interpretation, *Geophysical Research Letter*, **20** (9), (1993), 831-834.

Duarte, R.M., Wozniak, E., Recondo, C., Cabo, C., Marquínez, J., and Fernández, S.: Estimation of surface roughness and stone cover in burnt soils using SAR images, *Catena*, **74**, (2008), 264–272.

Evans, D.L., Farr, T.G., and van Zyl, J. J.: Estimates of surface roughness derived from Synthetic Aperture Radar (SAR) data, *IEEE Transaction Geoscience Remote Sensing*, **30**(2), (1992), 370–381.

Farr, T.G.: Microtopographic evolution of lava flows at Cima volcanic field, Mojave Desert, California. *Journal of Geophysical Research*, **97**(B11), (1992), 15171 – 15179.

Farr, T.G., Rosen, P.A., Caro, E., Crippen, R., Duren, R., Hensley, S., Kobrick, M., Paller, M., Rodriguez, E., Roth, L., Seal, D., Shaffer, S., Shimada, J., Umland, J., Werner, M., Oskin, M., Burbank, D., and Alsdorf, D.: The Shuttle Radar Topography Mission, *Reviews of Geophysics*, **45**, (2007).

Gaddis, L.R.P, Mouginis-Mark, P.J., and Hayashi, J.N.: Lava flow surface textures - SIR-B radar image texture, field observations, and terrain measurements, *Photogrammetric Engineering and Remote Sensing*, **56**, (1990), 211–224.

Gherardi, F., Panichia, C., and Yock A., Gerardo-Abaya, J.: Geochemistry of the surface and deep fluids of the Miravalles volcano geothermal system (Costa Rica), *Geothermics*, **31**, (2002), 91–128.

Joseph, E.P., Fournier, N., Lindsay, J.M., Robertson, R., and Beckles, D.M.: Chemical and isotopic characteristics of geothermal fluids from Sulphur Springs, Saint Lucia, *Journal of Volcanology and Geothermal Research*, **254**, (2013), 23–36.

Libbey, R.B. and Williams-Jones, A.E.: Relating sulfide mineral zonation and trace element chemistry to subsurface processes in the Reykjanes geothermal system, Iceland, *Journal of Volcanology and Geothermal Research*, **310**, (2016), 225–241.

Saepuloh, A., Koike, K., Omura, M., Iguchi, M., and Setiawan, A.: SAR- and gravity change-based characterization of the distribution pattern of pyroclastic flow deposits at Mt. Merapi during the past ten years, *Bulletin of Volcanology*, **72**(2), (2010), 221-232.

Saepuloh, A., Koike, K., and Omura, M.: Applying Bayesian decision classification to Pi-SAR polarimetric data for detailed extraction of the geomorphologic and structural features of an active volcano, *IEEE Geoscience and Remote Sensing Letters (GRSL)*, **99**(4), (2012), 554-558.

Saepuloh, A., Koike, K., Urai, M., and Sri Sumantyo, J.T.: Identifying surface materials on an active volcano by deriving dielectric permittivity from polarimetric SAR data, *IEEE Geoscience and Remote Sensing Letters (GRSL),* **12**(8), (2015), 1620-1624.

Shimada, M., Isoguchi, O., Tadono, T., Higuchi, R., and Isono, K.: PALSAR CALVAL Summary (JAXA-PI193), *Proceedings*. The First Joint PI Symposium of ALOS Data Nodes for ALOS Science Program, Kyoto, Japan (2007).

Whittaker, J.M., Muller, R.D., Sdrolias, M., Heine, C.: Sunda-Java trench kinematics, slab window formation and overriding plate deformation since the Cretaceous, *Earth and Planetary Science Letter*, **225**, (2007), 445–457.